JOURNAL OF BACTERIOLOGY, Jan. 2009, p. 320–332 Vol. 191, No. 1
0021-9193/09/$08.00+0 doi:10.1128/JB.00858-08
Copyright © 2009, American Society for Microbiology. All Rights Reserved.

Genetic Interactions of *smc*, *ftsK*, and *parB* Genes in *Streptomyces coelicolor* and Their Developmental Genome Segregation Phenotypes▽†

Rebekah M. Dedrick, Hans Wildschutte,‡ and Joseph R. McCormick*

Department of Biological Sciences, Duquesne University, Pittsburgh, Pennsylvania 15282

Received 23 June 2008/Accepted 21 October 2008

The mechanisms by which chromosomes condense and segregate during developmentally regulated cell division are of interest for *Streptomyces coelicolor*, a sporulating, filamentous bacterium with a large, linear genome. These processes coordinately occur as many septa synchronously form in syncytial aerial hyphae such that prespore compartments accurately receive chromosome copies. Our genetic approach analyzed mutants for *ftsK*, *smc*, and *parB*. DNA motor protein FtsK/SpoIIIE coordinates chromosome segregation with septum closure in rod-shaped bacteria. SMC (*s*tructural *m*aintenance of *c*hromosomes) participates in condensation and organization of the nucleoid. ParB/Spo0J partitions the origin of replication using a nucleoprotein complex, assembled at a centromere-like sequence. Consistent with previous work, we show that an *ftsK*-null mutant produces anucleate spores at the same frequency as the wild-type strain (0.8%). We report that the *smc* and *ftsK* deletion-insertion mutants (*ftsK′* truncation allele) have developmental segregation defects (7% and 15% anucleate spores, respectively). By use of these latter mutants, viable double and triple mutants were isolated in all combinations with a previously described *parB*-null mutant (12% anucleate spores). *parB* and *smc* were in separate segregation pathways; the loss of both exacerbates the segregation defect (24% anucleate spores). For a triple mutant, deletion of the region encoding the FtsK motor domain and one transmembrane segment partially alleviates the segregation defect of the *smc parB* mutant (10% anucleate spores). Considerable redundancy must exist in this filamentous organism because segregation of some genomic material occurs 90% of the time during development in the absence of three functions with only a fourfold loss of spore viability. Furthermore, we report that *scpA* and *scpAB* mutants (encoding SMC-associated proteins) have spore nucleoid organization defects. Finally, FtsK-enhanced green fluorescent protein (EGFP) localized as bands or foci between incipient nucleoids, while SMC-EGFP foci were not uniformly positioned along aerial hyphae, nor were they associated with every condensing nucleoid.

Streptomyces coelicolor is a filamentous sporulating soil saprophyte and it is the best-characterized model organism for an important group of bacteria known for their elaborate life cycle and their production of biologically active compounds. During the culmination of their life cycle, streptomycetes make chains of unicellular, metabolically quiescent reproductive cells that subsequently separate for dispersion and long-term survival in the environment (13). The genome of *S. coelicolor* is a large 8.7-Mb linear molecule with a centrally located *oriC* region, ending with long terminal inverted repeats (TIRs) (3). An aging surface-grown *Streptomyces* colony contains two basic zones of filamentous cells with different cytological properties (15). The vegetative mycelium contains branching syncytial hyphae, where the genome copies are not segregated or condensed into nucleoids and septation is infrequent and unevenly spaced. In contrast, the aerial mycelium contains mostly unbranched syncytial aerial hyphae, and within a given hypha, uniformly spaced septation synchronously occurs to form a chain of spores, each with a highly condensed nucleoid. Coincident with the synchronous septation, dozens of dispersed copies of the genome are accurately partitioned and condensed in the forming unicellular spores. It is conceivable that these synchronous processes coordinating the accurate separation of multiple copies of a linear genome may require a special or augmented system of segregation and condensation.

Condensation and segregation of the genome is a subject of great interest in microbial cell biology. Most of the known information has come from the study of bacterial cells that undergo binary fission (14, 51). These bacterial models typically have a single circular chromosome that is compacted into a nucleoid, and genome segregation occurs simultaneously with DNA replication. In rod-shaped bacteria, three well-characterized systems dovetail to ensure that chromosomes are equally and faithfully partitioned to daughter cells. FtsK (SpoIIIE), SMC (*s*tructural *m*aintenance of *c*hromosomes; functional homologue, MukB in *Escherichia coli*), and ParAB (Soj-Spo0J) have been identified as key players. First, FtsK/SpoIIIE homologues are well-studied sequence-directed DNA motor proteins that localize at the invaginating septa and clear each genome copy to the appropriate side of the septum during vegetative growth and sporulation (references 2, 6, 23, and 42 and references therein). The homologues typically have an N-terminal domain with membrane-spanning segments responsible for septal localization separated by a linker from a more highly conserved C-terminal motor protein domain (34). Second, SMC proteins are widely distributed from bacteria to mammals and participate in higher levels of chromatin orga-

* Corresponding author. Mailing address: Department of Biological Sciences, Duquesne University, Pittsburgh, PA 15282. Phone: (412) 396-4775. Fax: (412) 396-5907. E-mail: mccormick@duq.edu.

† Supplemental material for this article may be found at http://jb.asm.org/.

‡ Present address: Department of Civil and Environmental Engineering, Massachusetts Institute of Technology, Cambridge, MA 02139.

▽ Published ahead of print on 31 October 2008.

nization, acting either as condensins or cohesins (references 18, 22, 38, and 50 and references therein). DNA may be pulled into the cell by the action of these proteins from a single site or a limited number of sites. The molecular details of how these large hinged proteins function in association with non-SMC modulators (ScpAB/MukEF) to compact the chromosome into higher-order structures are being determined (8, 9, 21). Third, chromosomes from a wide range of bacteria use a partition system related to ones described for certain low-copy-number plasmids. Two *trans*-acting factors, ParA (Soj) ATPase and ParB (Spo0J), and *cis*-acting *parS* ("centromere") sites in the origin-proximal region are utilized (references 5, 12, and 51 and references therein). Spo0J (ParB) binds to the *parS* sites to form a large nucleoprotein complex that can spread beyond the origin region (7). ParA is required for the proper placement of the ParB-*parS* nucleoprotein complex in the cell. For unicellular bacteria, individual inactivation of any of these three systems results in a severe segregation phenotype, and combining them typically leads to synthetic lethal phenotypes.

How copies of the linear genome are synchronously partitioned during sporulation in *S. coelicolor* is beginning to be appreciated. If utilized, the physical landmarks in the apical aerial hypha, the tip (pole) and the septum at the base of the long apical cell, can be separated by 40 to 50 μm or more. DNA segregation occurs after active rounds of DNA replication populate the predivisional apical cell with several dozen dispersed copies of the genome (44). After DNA replication ceases, septa synchronously form over these unsegregated copies of the genome (37, 46, 54). ParB binds to about 20 *parS* sites densely packed around *oriC* in the chromosome, forming a nucleoprotein complex that helps to accurately partition the chromosome during division (24, 28). ParB-enhanced green fluorescent protein (EGFP) localizes as regularly spaced foci assembled along aerial hyphae before DNA segregation and septation begin, suggesting that the origin region of the chromosome is accurately positioned between where adjacent septa form (25). ParA assembles into helical structures along aerial hyphae to facilitate the organization of evenly spaced ParB-*oriC* complexes (26). It was anticipated that the FtsK motor protein would be instrumental in ensuring that the genomic DNA trapped by invaginating septa would be properly partitioned; however, strains containing a complete deletion of *ftsK* resulted in a mild segregation phenotype (1, 53). SffA, another FtsK/SpoIIIE-like protein, localizes to sporulation septa and may function in chromosomal DNA organization during differentiation (1). Septal localization of SffA requires a small protein called SmeA, which itself appears to have a more pleiotropic role in spore maturation. Thus, progress has been made, but there are still substantial gaps in our understanding of how the linear genome is segregated and condensed.

In this study, we evaluated the functions of *ftsK* and *smc* in *S. coelicolor* by constructing *ftsK* and *smc* deletion-insertion mutant strains. In contrast to what was found in two recent studies, the *ftsK* allele reported here results in a C-terminal truncation, removing the DNA motor domain of FtsK and a membrane-spanning segment. Each mutation studied here was found to affect the accuracy of genome segregation into spores. We then extended our analysis using a previously published *parB* mutation. We report that all double and triple mutants are viable. Surprisingly, the majority of the spores produced by a triple mutant still receive genomic material with a modest fourfold decrease in viability, suggesting that there are additional genes responsible for proper developmental genome segregation and condensation. In addition, we show that mutations in the genes encoding SMC-associated proteins ScpA and ScpB mainly affect the nucleoid morphology in prespore compartments rather than impairing segregation. Finally, we determined the subcellular localization of FtsK and SMC in aerial hyphae undergoing differentiation using EGFP translational fusions.

MATERIALS AND METHODS

Bacterial strains and media. *S. coelicolor* A3(2) strains used in this study are listed in Table 1. YEME (liquid), R2YE (agar), MS (agar), and minimal medium (MM; agar with 0.5% glucose [wt/vol]) were used for growth of *S. coelicolor* at 30°C (27, 36). Standard procedures for protoplast preparation and transformation were used (27). Antibiotics used for *S. coelicolor* were as follows: apramycin at 25 μg ml^{-1}, neomycin at 10 μg ml^{-1}, hygromycin at 200 μg ml^{-1}, kanamycin at 160 μg ml^{-1}, and thiostrepton at 50 μg ml^{-1}. The viability of the wild type and of certain mutant strains was determined using the average of at least two independent spore preparations (growth on MS) analyzed from duplicate serial dilutions by direct count using phase-contrast microscopy and viable count after 3 days of incubation on glucose MM.

E. coli strain TG1 was used for standard plasmid manipulation (45). *E. coli* strain BW25113 containing λ RED plasmid pIJ790 (19) was used for in vivo construction of *egfp* fusions or deletion of *scpAB*. *E. coli* strain ET12567 (*dam dcm hsdM*) (31) was used to prepare unmodified plasmid and cosmid DNA to circumvent the restriction system of *S. coelicolor*. Final concentrations of antibiotics in LB medium used for *E. coli* were as follows: for ampicillin, 100 μg ml^{-1}; for carbenicillin, 100 μg ml^{-1}; for apramycin, 100 μg ml^{-1}; for chloramphenicol, 25 μg ml^{-1}; and for kanamycin, 50 μg ml^{-1}.

Plasmids and general DNA techniques. Plasmids used in this study are listed in Table 2. *S. coelicolor* total DNA preparations were obtained using the Wizard genomic DNA purification kit (Promega). DNA restriction and modifying enzymes were used according to the manufacturer's recommendation (New England BioLabs). *Taq* (Promega) and *Pfx* (Invitrogen) DNA polymerases were used according to the manufacturer's instructions. Redirect technology (19) was used for λ RED-mediated recombination using mutagenic linear DNA cassettes in *E. coli*.

Isolation of *ftsK* insertion-deletion mutant strains. Insertion-deletion mutations for *ftsK* of *S. coelicolor* were constructed in *E. coli* by use of traditional in vitro recombinant DNA technology. In plasmids pJR148 and pJR152 (Table 2), 1.8 kb of the 3′ end of the *ftsK* gene, encoding the DNA motor domain and one membrane-spanning segment, was replaced by a neomycin resistance marker (*aphI*), inserted in either orientation. The insertion-deletion mutations in pJR148 and pJR152 were introduced into the chromosome by transformation, selecting for neomycin resistance and screening for apramycin sensitivity. Two independent representative strains were named JM148 and JM152, respectively. These strains could express a C-terminally truncated version of FtsK containing the first 203 amino acids (out of 929). In plasmid pAEB232 (Table 2), a 2.5-kb deletion, beginning 57 bases upstream of the translation start site and ending at the same position as described above, results in the entire 5′ end of the *ftsK* gene being replaced by an apramycin resistance marker [*acc(3)IV*]. The insertion-deletion mutation in pAEB232 was introduced into the *S. coelicolor* chromosome by transformation, selecting for apramycin resistance and screening for spectinomycin sensitivity. The resulting strain RMD24 should not express FtsK.

Isolation of *smc* deletion-insertion mutant strains. Insertion-deletion mutations in *smc* of *S. coelicolor* were constructed in *E. coli* by use of traditional in vitro recombinant DNA technology. Initially, we isolated a Δ*smc*::*acc(3)IV* mutant (strain HW1) to determine that the *smc* gene was dispensable (55). We isolated another *smc*-null strain, containing Δ*smc*::*hyg*, for compatibility with other mutation markers used in this study. In plasmid pHJ2 (Table 2), the majority of *smc* was replaced by a hygromycin resistance gene (*hyg*). By use of pHJ2, the Δ*smc*::*hyg* mutation was introduced into the *S. coelicolor* chromosome by transformation, selecting for hygromycin resistance and screening for apramycin sensitivity. One representative strain was named HJ2.

Characterization of a *parB* mutant strain. Strain J2537 [Δ*parB*::*acc(3)IV*] strain was a gift from Keith Chater (28). By Southern blot hybridization analysis, we determined that the apramycin resistance gene was in the same orientation as *parB*.

TABLE 1. *S. coelicolor* A3(2) strains used in this study

Strain	Genotype[a]	Isolation[b]	Reference or source
2709	*proA1 hisA1 argA1 cysD18 uraA1 strA1* SCP1$^-$ SCP2$^-$		27
HJ2	Δ*smc*::*hyg*	M145 × pHJ2	This study
J2537	Δ*parB*::*acc(3)IV*		28
J2540	Δ*parB*::*acc(3)IV*/*parB*$^+$	J2537::pIJ6539	28
JM148	Δ*ftsK*::*aphI* (*aphI* inserted in same orientation as *ftsK′*)	M145 × pJM148	This study
JM152	Δ*ftsK*::*aphI* (*aphI* inserted in opposite orientation from *ftsK′*)	M145 × pJM152	This study
M145	Prototroph SCP1$^-$ SCP2$^-$		27
RMD1	*ftsK-egfp acc(3)IV*	M145 × 7C7*ftsK-egfp*	This study
RMD2	*smc-egfp acc(3)IV*	M145 × 7A1*smc-egfp*	This study
RMD3	Δ*smc*::*hyg* Δ*ftsK*::*aphI*	HJ2 × JM148	This study
RMD4	Δ*smc*::*hyg* Δ*parB*::*acc(3)IV*	HJ2 × J2537	This study
RMD5	Δ*parB*::*acc(3)IV* Δ*ftsK*::*aphI*	J2537 × JM148	This study
RMD6	Δ*smc*::*hyg* Δ*parB*::*acc(3)IV* Δ*ftsK*::*aphI*	RMD3 × J2537	This study
RMD7	Δ*smc*::*hyg*/*smc*$^+$	HJ2/pHW35	This study
RMD8	Δ*ftsK*::*aphI*/*ftsK*$^+$	JM148/pRMD6	This study
RMD9	Δ*smc*::*hyg* Δ*ftsK*::*aphI*/*ftsK*$^+$	RMD3/pRMD6	This study
RMD10	Δ*smc*::*hyg* Δ*ftsK*::*aphI*/*smc*$^+$	RMD3/pHW35	This study
RMD11	Δ*smc*::*hyg* Δ*parB*::*acc(3)IV*/*smc*$^+$	RMD4/pHW35	This study
RMD12	Δ*smc*::*hyg* Δ*parB*::*acc(3)IV*/*parB*$^+$	J2540 × HJ2	This study
RMD13	Δ*parB*::*acc(3)IV* Δ*ftsK*::*aphI*/*ftsK*$^+$	RMD5/pRMD6	This study
RMD14	Δ*parB*::*acc(3)IV* Δ*ftsK*::*aphI*/*parB*$^+$	J2540 × RMD5	This study
RMD15	Δ*smc*::*hyg* Δ*parB*::*acc(3)IV* Δ*ftsK*::*aphI*/*ftsK*$^+$	RMD6/pRMD6	This study
RMD16	Δ*smc*::*hyg* Δ*parB*::*acc(3)IV* Δ*ftsK*::*aphI*/*smc*$^+$	RMD6/pHW35	This study
RMD17	ΔSCO1768::*acc(3)IV*	M145 × pRMD7	This study
RMD18	Δ*scpA*::*acc(3)IV*	M145 × pRMD8	This study
RMD19	Δ*scpAB*::*acc(3)IV*	M145 × pRMD9	This study
RMD20	Δ*smc*::*hyg* Δ*scpA*::*acc(3)IV*	HJ2 × RMD18	This study
RMD21	Δ*smc*::*hyg* Δ*scpAB*::*acc(3)IV*	HJ2 × RMD19	This study
RMD22	Δ*scpA*::*acc(3)IV*/*scpAB*$^+$	RMD18/pRMD10	This study
RMD23	Δ*scpAB*::*acc(3)IV*/*scpAB*$^+$	RMD19/pRMD10	This study
RMD24	Δ*ftsK*::*acc(3)IV* (null, deletion begins upstream of 5′ end)	M145 × pAEB232	This study

[a] All mutants are derivatives of prototrophic strain M145.
[b] Strains were constructed by protoplast transformation: the recipient strain is listed first and the source of donor DNA second (e.g., HJ2 × JM148 indicates that HJ2 was transformed with DNA prepared from JM148), or the recipient strain is listed first and the mutagenic plasmid second (e.g., M145 × pHJ2).

Isolation of *scpA* and *scpAB* mutants. Insertion-deletion mutations in SCO1768, *scpA*, and *scpB* of *S. coelicolor* were constructed in vivo in *E. coli* by use of λ RED-mediated recombination and cosmid SCI51. In cosmid derivatives pRMD7, pRMD8, and pRMD9, the majority of the SCO1768 (encoding a putative pseudouridine synthase), *scpA*, and *scpAB* genes, respectively, were replaced by a cassette obtained from pIJ773, containing an apramycin resistance gene and *oriT* flanked by FRT sites (19). Oligonucleotides listed in Table 3 were used as primers in PCRs to add homology to the ends of the apramycin resistance gene cassette. Primers 60Sco1768 and 59Sco1768 were used for completely deleting SCO1768, oScpA60 and oScpA59 were used for deleting the middle 777 bases of the 792-base *scpA*, and oScpA60 and oScpB59 were used for deleting *scpA* and the first 426 bases of the 5′ end of the 672-base *scpB*. The insertion-deletion mutations in each of the cosmids were introduced into the chromosome by conjugation, selecting for apramycin resistance and screening for kanamycin sensitivity. Representative strains were named RMD17 [ΔSCO1768::*acc(3)IV*], RMD18 [Δ*scpA*::*acc(3)IV*], and RMD19 [Δ*scpAB*::*acc(3)IV*].

Isolation of double and triple mutant strains. Double and triple mutant strains were constructed using protoplasts prepared from one mutant strain and transforming with chromosomal DNA prepared from a second mutant strain (Table 1). All double and triple mutant strains were readily isolated by selection using the antibiotic resistance gene marking each insertion-deletion mutation.

Southern blot hybridization analysis. Each mutation in single, double, and triple deletion-insertion mutant strains was confirmed by Southern blot hybridization analysis. Descriptions of probes used and data obtained are located in the supplementary material. Hybridization reactions were performed at 65°C using buffer that contained 5% sodium dodecyl sulfate (52). Nylon membranes (Hybond-N; Amersham) were used as solid support, and probes were nonisotopically labeled before immunological detection (digoxigenin DNA labeling and detection kit; Boehringer Mannheim).

Construction of plasmids for genetic complementation. Genetic complementation plasmids were derived from the self-transmissible, low-copy-number, bifunctional plasmid pJRM10 (Table 2). *ftsK*$^+$ is the only complete reading frame on the DNA insert of plasmid pRMD6. *smc*$^+$ is the only complete reading frame on the DNA insert of plasmid pHW35. The DNA insert of *scpAB* complementation plasmid pRMD11 contains five complete genes: SCO1772, SCO1771 (hypothetical gene), *scpAB*$^+$, and the downstream gene SCO1768 (putative pseudouridine synthase). The insert in pRMD11 ends 1 base downstream of SCO1768. These plasmids were introduced into the multiple auxotroph 2709 by transformation, selecting for thiostrepton resistance. The plasmids were mated from the 2709 derivative into the desired mutant strains, selecting for thiostrepton resistance and prototrophy. Transconjugants were tested for the presence of the antibiotic resistance genes marking the chromosomal mutations.

Strain J2540 (Δ*parB*/*parB*$^+$) and derivatives isolated here had *parB*$^+$ integrated by single homologous crossover recombination using plasmid pIJ6539 (28).

Construction of strains expressing EGFP fusion proteins. Genes expressing EGFP fusions were constructed in one step by in vivo recombination. Cosmid H24*parB-egfp* (25) was used as the source of an *egfp acc(3)IV oriT* cassette to make *ftsK-egfp* and *smc-egfp* fusions. PCR was performed using H24*parB-egfp* as the template with specific oligonucleotides which anneal to the linker sequence at the 5′ end of *egfp* and downstream of the 3′ end of *acc(3)IV* and introduce 40 bases of homology to the 3′ ends of *smc* or *ftsK*, as well as removing the stop codons (Table 3). PCR products were introduced into *E. coli* strains expressing λ RED recombination functions and containing the cognate cosmid with either *ftsK* (SC7C7) or *smc* (SC7A1). Apramycin-resistant transformants were selected creating 7C7*ftsK-egfp* and 7A1*smc-egfp*. The gene fusion junction and *egfp* sequences were verified. The proline- and glycine-rich 5-amino-acid linker peptide (LPGPE) was similar to that of H24*parB-egfp* (25). Fusion-containing cosmids were conjugated from *E. coli* into strain M145, selecting for apramycin resistance and kanamycin sensitivity. In these transconjugants (RMD1 and RMD2), the fusion genes (*ftsK-egfp* and *smc-egfp*, respectively) are the only copies of *ftsK* or *smc*.

Microscopy. Strains were characterized by confocal laser scanning microscopy using a Leica SP2 microscope equipped with a phase-contrast 100× oil objective

TABLE 2. Plasmids and cosmids used in this study

Plasmid	Description	Reference or source
SC7A1	Cosmid source of *smc*	43
SC7C7	Cosmid source of *ftsK*	43
SCI51	Cosmid source of *scpAB*	43
H24*parB-egfp*	*egfp* inserted in frame 3′ of *parB* in cosmid SCH24; *acc(3)IV aphII*	25
7A1*smc-egfp*	*egfp* inserted in frame 3′ of *smc* in cosmid SC7A1; *acc(3)IV aphII*	This study
7C7*ftsK-egfp*	*egfp* inserted in frame 3′ of *ftsK* in cosmid SC7C7; *acc(3)IV aphII*	This study
pAEB228	4.2-kb PvuII fragment from SC7C7 containing *ftsK* cloned into EcoRV-digested pBluescript (*ftsK*; same orientation as *lacZ′*)	This study
pAEB232	2.5-kb MluI-SphI deletion of pJR143 [Δ*ftsK*::*acc(3)IV*; same orientation as *ftsK*]; *aadA*	This study
pAH137	Source of neomycin resistance gene *aphI*	A. Hausler, unpublished data
pBluescriptII SK(+)	Standard cloning vector	Stratagene
pIJ773	Source of *acc(3)IV* for in vivo recombination	19
pIJ6539	5.3-kb EcoRI fragment containing *parB*; *tsr* (*parB* complementation plasmid)	28
pKC1053	Source of hygromycin resistance gene *hyg*	29
pHJ2	3.2-kb SalI-PstI deletion of pHW25 (Δ*smc*::*hyg*; same orientation as *smc*); *acc(3)IV*	This study
pHW24	5.4-kb XhoI fragment from SC7A1 cloned into pBluescript (*smc*; opposite orientation from *lacZ′*)	This study
pHW25	5.4-kb XhoI fragment from SC7A1 cloned into pBluescript (*smc*; same orientation as *lacZ′*)	This study
pHW35	24-kb BamHI-EcoRI fragment from pJRM10 cloned into pHW24 (*smc* complementation plasmid)	This study
pJR143	6.1-kb BamHI-PstI fragment of SC7C7 containing *ftsK* cloned into pOJ260 (*ftsK*; same orientation as *lacZ′*); *acc(3)IV*	This study
pJR148	1.8-kb SphI fragment deletion of pJR143 (Δ*ftsK*::*aphI*; same orientation as *ftsK′*); *acc(3)IV*	This study
pJR152	1.8-kb SphI fragment deletion of pJR143 (Δ*ftsK*::*aphI*; opposite orientation from *ftsK′*); *acc(3)IV*	This study
pJRM10	Bifunctional cloning vector, low copy number in *S. coelicolor*; *bla tsr*	35
pOJ260	pUC-like plasmid containing *oriT* and *acc(3)IV* in place of *bla*	4
pOJ427	Source of apramycin resistance gene *acc(3)IV* for in vitro recombination	B. Schoner, unpublished data
pRMD6	24-kb EcoRI-HindIII fragment from pJRM10 cloned into pAEB228 (*ftsK* complementation plasmid)	This study
pRMD7	Cosmid SCI51 containing Δ*SCO1768*::*acc(3)IV* by in vivo recombination; *aphII*	This study
pRMD8	Cosmid SCI51 containing Δ*scpA*::*acc(3)IV* by in vivo recombination; *aphII*	This study
pRMD9	Cosmid SCI51 containing Δ*scpAB*::*acc(3)IV* by in vivo recombination; *aphII*	This study
pRMD10	4.8-kb XbaI fragment from SCI51 containing *scpAB* cloned into pBluescript (*scpAB*; opposite orientation from *lacZ′*)	This study
pRMD11	24-kb HindIII-SpeI fragment from pJRM10 cloned into pRMD10 (*scpAB* complementation plasmid)	This study

(numerical aperture, 1.40) and 488- and 543-nm lasers. Autofluorescence seen in wide-field microscopy is not an issue with confocal microscopy with appropriately adjusted excitation light. There was no background autofluorescence in the wild-type strain under the conditions used. Standardized amounts of spores (CFU) were inoculated on MS agar adjacent to sterile coverslips that were embedded at a 45° angle in the agar medium and incubated for the indicated lengths of time. Coverslips were removed and cell material was fixed at room temperature for 10 min using a phosphate-buffered saline solution containing 4.375% glutaraldehyde and 0.028% paraformaldehyde. The coverslips were washed twice with phosphate-buffered saline, allowed to air dry, and mounted in 50% glycerol containing 0.1% propidium iodide, a total nucleic acid stain. Images were processed to adjust the brightness and contrast using Adobe Photoshop and assembled in Adobe Illustrator.

Computer analysis. Predicted gene and protein products were obtained from the *S. coelicolor* genome database StrepDB (http://streptomyces.org.uk/).

RESULTS

Identification of *ftsK* and *smc* homologues in *S. coelicolor*. FtsK (SpoIIIE) is a DNA motor protein that is involved in the process of chromosome partitioning during cell division or spore formation (30, 57, 59). The *ftsK* (SCO5750) gene is 2,790 bp and is predicted to encode a 929-amino-acid protein, $FtsK_{Sc}$ (Fig. 1A). Complementing our study, recently published articles also reported genetic analysis of SCO5750 (1, 53). Transmembrane prediction program analyses for $FtsK_{Sc}$ are consistent with the models containing four transmembrane domains proposed for $SpoIIIE_{Bs}$ (56) and $FtsK_{Ec}$ (11). The N terminus is required for targeting FtsK to the division plane (53).

SMC proteins are extremely well conserved throughout prokaryotes, archaea, and eukaryotes; they are involved in chromosome maintenance and structure (21a, 28b, 50a). The *smc* gene of *S. coelicolor* (SCO5577) is 3,561 bp in length and is predicted to encode a 1,186-amino-acid protein (Fig. 1B). SMC proteins consist of N- and C-terminal DNA-binding domains connected by two coiled-coil regions joined by a hinge. The highest similarities to homologues were in the N- and C-terminal ATPase domains (54% and 46% identical to SMC of *Bacillus subtilis*, respectively). The functional analogue of SMC is MukB in *E. coli*.

***ftsK* and *smc* are dispensable for growth and viability of *S. coelicolor*.** Plasmids pJR148 and pJR152 were constructed in vitro and contain a deletion-insertion mutation for *ftsK* marked with a neomycin resistance gene (Δ*ftsK*::*aphI*), with *aphI*

TABLE 3. Oligonucleotides used in this study

Oligonucleotide	Sequence[a]	Application
oSMCgfpF	CGGTGTGTCGAAGGTCATCAGCCAGCGGTTGCGTCAGCCCCTGCCGG GCCCGGAGCTG	Construction of *smc-egfp*
oSMCgfpR	GAAGTGGTTATGTGTTCAAGTCTTGAAGAACGAGGGTTCACATATGT AGGCTGGAGCTGCTTC	Construction of *smc-egfp*
oKgfpF	GGACGGCGTGCTCGCGGTGATCCGTGGGGAGTCTGAAGGGCTGCCG GGCCCGGAGCTG	Construction of *ftsK-egfp*
oKgfpR	CGGCGGATCGTCGGCGGAACCCTTCTCCTACCCGCCCCTACATATGT AGGCTGGAGCTGCTTC	Construction of *ftsK-egfp*
60Sco1768	CCGGGGACGCAGACGACAAGACGGAATTTTG**ATG**CGAAGCATTCCG GGGATCCGTCGACC	Construction of Δ*SCO1768*::*acc(3)IV*
59Sco1768	TCGTCGGGGCAGGGGTTGCCCAGAGGCCGGT**CTA**GAGGTCTGTAGG CTGGAGCTGCTTC	Construction of Δ*SCO1768*::*acc(3)IV*
oScpA60	CTCCGACGACCCGGACGACGGTGTCTTCAAG**GTG**CGGCTCATTCCGG GGATCCGTCGACC	Construction of Δ*scpA*::*acc(3)IV*
oScpA59	GTGGCCTCCTCGGCCTCCGTGATCCGCTCAC**TCA**CGCCTTTGTAGGCT GGAGCTGCTTC	Construction of Δ*scpA*::*acc(3)IV*
oScpB59	TGCCCGCCTCCTCGACCAGACCCCGCTGCAGGAGGGTGCGTGTAGGC TGGAGCTGCTTC	Construction of Δ*scpAB*::*acc(3)IV*

[a] Start codons and reverse complements of stop codons are in boldface.

cloned in each orientation. The altered *ftsK* genes (*ftsK′*) can express a C-terminally truncated protein of 203 amino acids (FtsK′). Mainly, the motor domain was lost as the truncation is in a loop between the final two predicted transmembrane segments. Plasmid pHJ2 contains a deletion-insertion mutation for *smc* marked with a hygromycin resistance gene (Δ*smc*::*hyg*). By use of these plasmids, the mutations were introduced into the chromosome by transformation. Marker replacement strains were readily isolated, indicating that these genes are not essential for growth or viability. Macroscopically, these strains looked very similar to the wild-type strain. They grew well and formed a robust, gray, aerial mycelium (Fig. 1D). As noticed in two recently published papers, strains containing Δ*ftsK* mutations showed increased colony heterogeneity upon plating (1, 53). The Δ*ftsK* strains reported here also had increased colony heterogeneity, as did the Δ*smc* strain.

These new strains were further characterized using confocal laser scanning microscopy. The DNA segregation phenotype

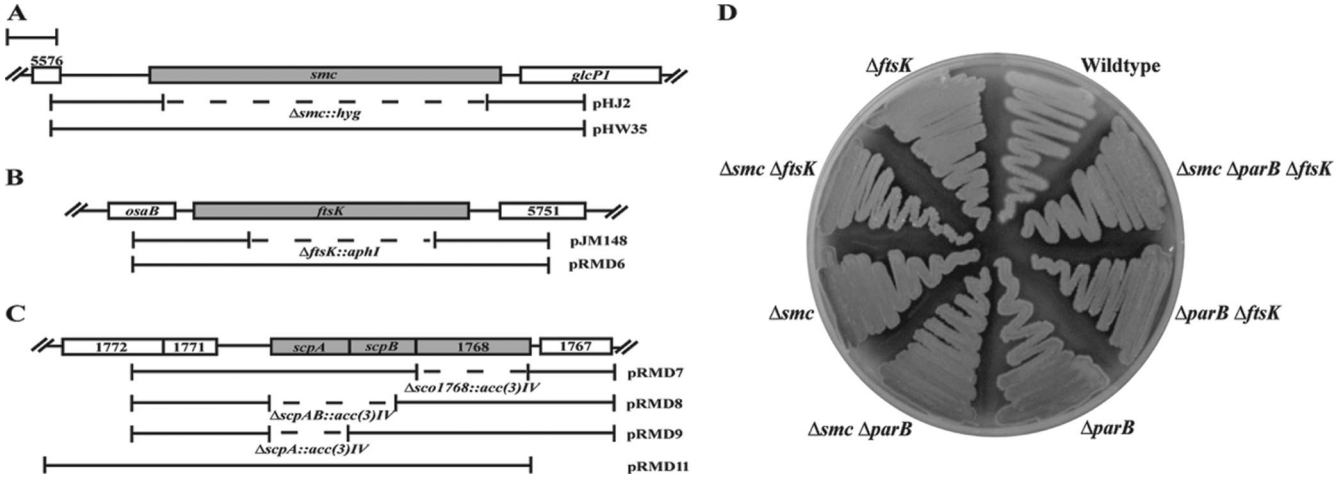

FIG. 1. Physical maps of regions of chromosomal DNA containing *smc*, *ftsK*, or *scpAB*. In each case, the flanking genes are in the same orientation as the genes of interest. Bar: 1 kb. (A) The *smc* region of the chromosome. SCO5576 is predicted to encode an acyl phosphatase and *glcP1* is involved in glucose uptake. For mutagenic plasmid pHJ2, the region deleted and replaced with a hygromycin resistance gene is shown (dashed line). The insert in complementation plasmid pHW35 is shown (bracketed line). (B) The *ftsK* region of the chromosome. *osaB* is part of a two-component regulator involved in osmoadaptation and SCO5751 is predicted to encode a hypothetical membrane protein. For mutagenic plasmid pJR148, the region of *ftsK* deleted and replaced with a neomycin resistance gene is shown (dashed line). The insert in complementation plasmid pRMD6 is shown (bracketed line). (C) The *scpAB* region of the chromosome. SCO1768, SCO1771, and SCO1767 are predicted to encode a pseudouridine synthase, a hypothetical protein found in actinomycetes, and a possible DNA hydrolase, respectively. For mutagenic cosmids pRMD7, -8, and -9, respectively, the regions of SCO1768, *scpA*, and *scpAB* deleted and replaced with an apramycin resistance gene are shown (dashed lines). The insert in complementation plasmid pRMD11 is shown (bracketed line); the DNA insert ends 1 base after SCO1768. (D) Single, double, and triple mutant strains macroscopically resemble the wild type. Strains were grown on MS agar for 4 days at 30°C. Mutant strains formed robust, gray-pigmented, aerial mycelia with no obvious growth or developmental delays. Strains M145 (wild type), J2537 (Δ*parB*), JM148 (Δ*ftsK*), HJ2 (Δ*smc*), RMD3 (Δ*smc* Δ*ftsK*), RMD4 (Δ*smc* Δ*parB*), RMD5 (Δ*parB* Δ*ftsK*), and RMD6 (Δ*smc* Δ*parB* Δ*ftsK*) are shown.

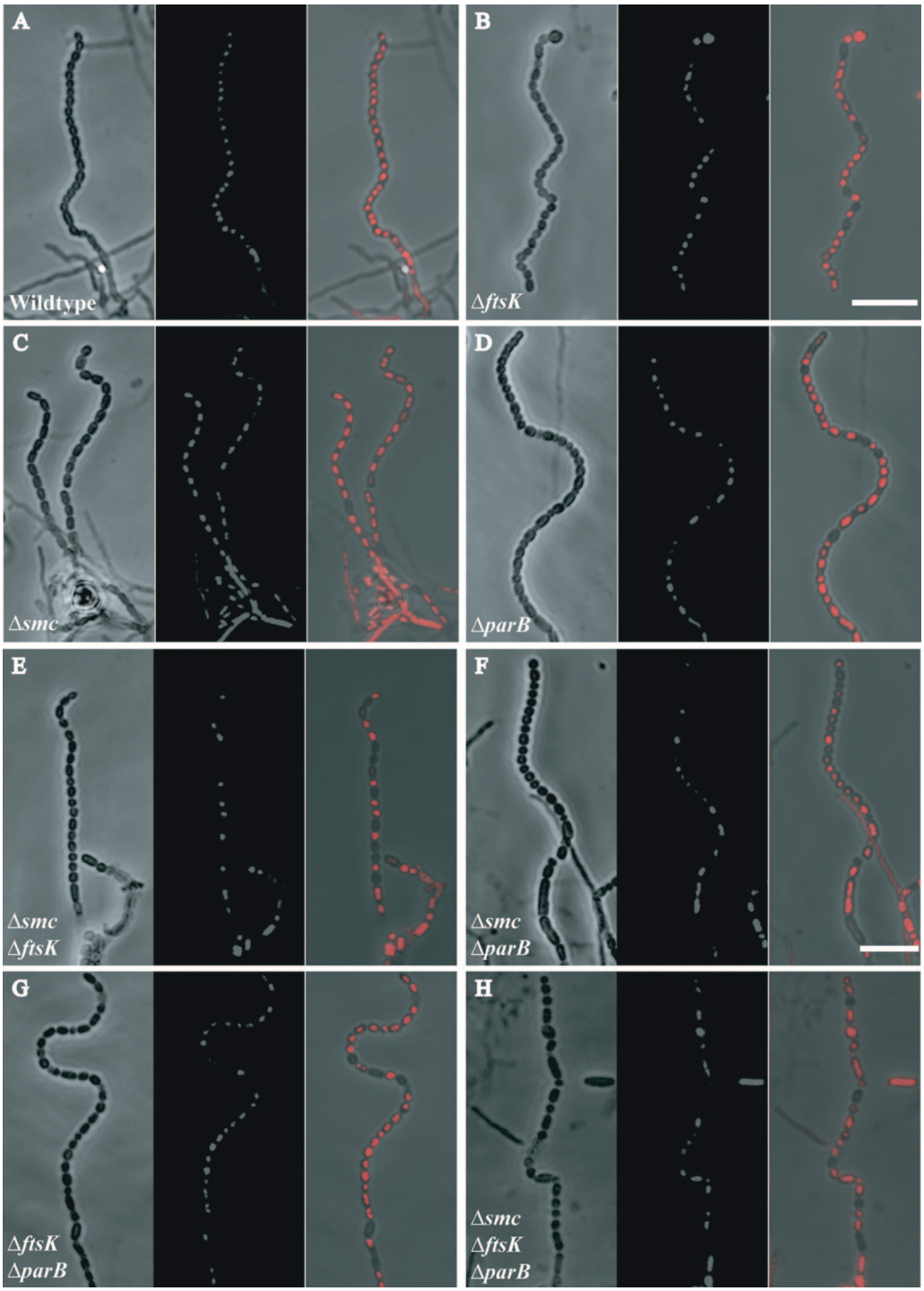

FIG. 2. Confocal microscope images showing sporulation and DNA segregation phenotypes of the wild type and of single, double, and triple mutant strains. Four-day-old cultures grown on MS agar were sampled on coverslips, fixed, and stained with propidium iodide (red). In each panel, phenotypes of representative aerial hyphae are shown as phase-contrast and fluorescent image pairs, followed by a merged image. (A) M145 (wild type). (B) JM148 (Δ*ftsK*). (C) HJ2 (Δ*smc*). (D) J2537 (Δ*parB*). (E) RMD3 (Δ*smc* Δ*ftsK*). (F) RMD4 (Δ*smc* Δ*parB*). (G) RMD5 (Δ*parB* Δ*ftsK*). (H) RMD6 (Δ*smc* Δ*parB* Δ*ftsK*). Bar: 7 μm.

associated with each mutant strain was determined by staining the DNA with propidium iodide. DNA segregation did not appear to be affected in vegetative hyphae of *ftsK* and *smc* mutants (data not shown). Figure 2 illustrates that spores formed in aerial hyphae in the single mutants (Fig. 2B to D) were similar to the wild type in shape and size (Fig. 2A) and had detectable defects in DNA partitioning (Table 4). The wild-type strain produced aerial hyphae with 0.8% anucleate

TABLE 4. Quantitative analysis of genome segregation defects during spore formation

Strain or mutation	% Anucleate spores[a]	Total no. of spores
Wild type	0.8	2,233
Δ*ftsK*::*acc(3)IV* (null)	0.8	1,876
Δ*ftsK*::*aphI* (*aphI* in same orientation as *ftsK′*)[b]	15	3,469
Δ*ftsK*::*aphI* (*aphI* in opposite orientation from *ftsK′*)	17	1,463
Δ*smc*::*hyg*	7	4,122
Δ*parB*::*acc(3)IV*	12	1,783
Δ*smc*::*hyg* Δ*ftsK*::*aphI*	13	2,389
Δ*smc*::*hyg* Δ*parB*::*acc(3)IV*	24	3,663
Δ*parB*::*acc(3)IV* Δ*ftsK*::*aphI*	13	3,230
Δ*smc*::*hyg* Δ*parB*::*acc(3)IV* Δ*ftsK*::*aphI*	10	1,503
Δ*smc*::*hyg*/*smc*$^+$	3	2,033
Δ*ftsK*::*aphI*/*ftsK*$^+$	5	2,180
Δ*smc*::*hyg* Δ*ftsK*::*aphI*/*ftsK*$^+$	7	2,008
Δ*smc*::*hyg* Δ*ftsK*::*aphI*/*smc*$^+$	11	1,667
Δ*smc*::*hyg* Δ*parB*::*acc(3)IV*/*smc*$^+$	14	1,809
Δ*smc*::*hyg* Δ*parB*::*acc(3)IV*/*parB*$^+$	6	1,807
Δ*parB*::*acc(3)IV* Δ*ftsK*::*aphI*/*ftsK*$^+$	16	2,009
Δ*parB*::*acc(3)IV* Δ*ftsK*::*aphI*/*parB*$^+$	18	2,125
Δ*smc*::*hyg* Δ*parB*::*acc(3)IV* Δ*ftsK*::*aphI*/*ftsK*$^+$	27	2,075
Δ*smc*::*hyg* Δ*parB*::*acc(3)IV* Δ*ftsK*::*aphI*/*smc*$^+$	11	1,712

[a] One hundred random spore chains were quantified and the percentages of anucleate spores were determined. All spores were considered regardless of the compartment size.

[b] Double and triple mutants contained this allele of *ftsK′*.

spores. Because of its similarity to eukaryotic condensins and cohesins, we anticipated a chromosome condensation defect in the Δ*smc* mutant, but no obvious phenotype was observed and nucleoids in mature spore compartments were no less condensed. The Δ*smc* mutant produced aerial hyphae with 7% anucleate spores, which indicated a defect in segregation. For the Δ*smc* mutant, we did not observe spores with trapped DNA inside the septa (guillotine effect) as was observed for the *E. coli mukB* mutant (39). Consistent with the gene product's role as a DNA motor protein, the Δ*ftsK* truncation mutants, isolated with different orientations of *aphI*, behaved similarly and produced aerial hyphae with 15 to 17% anucleate spores (Table 4). Here, for certain hyphae, we did observe DNA trapped in septa and small spore compartments with less DNA than normal (data not shown). The observed segregation defect was surprising, because complete deletions of *ftsK* resulted in strains that produced spores with reduced DNA staining but no anucleate spores (1, 53). To rule out a difference in laboratory copies of the same wild type, we isolated a strain containing a complete deletion of *ftsK* [RMD24; Δ*ftsK*::*acc*(*3*)*IV*] and observed that it produced anucleate spores at a level similar to that seen for the wild-type parent (Table 4), in agreement with the other recent studies. We concluded that expressing the truncated version, FtsK′, was responsible for anucleate spore production in the Δ*ftsK*::*aphI* strains (JM148 and JM152). For comparison, we analyzed the previously published Δ*parB* mutant (28). Analysis of the Δ*parB* strain under our growth conditions indicated that it produced aerial hyphae with 12% anucleate spores (Table 4), the same level as was originally reported. Thus, loss of *parB* or the portion of *ftsK* encoding the DNA motor domain and a membrane-spanning segment had a similar effect on the fidelity of simultaneous DNA segregation into each prespore compartment. The effect of losing *smc* was more modest, i.e., about half that observed for the loss of *parB* or the truncation of *ftsK*. Completely removing *ftsK* had no effect on anucleate spore production.

Genetic complementation experiments were completed to confirm that the segregation phenotypes observed were due to the truncation of *ftsK* or the loss of *smc* and not to an unlinked mutation. Wild-type copies of each gene were cloned into the low-copy-number vector pJRM10 (SCP2* derivative; one or two copies/chromosome). The DNA inserts contained only one complete gene, *ftsK* or *smc* (Fig. 1A and B). The phenotypes of the complemented Δ*ftsK* and Δ*smc* mutants were analyzed (Table 4). The Δ*ftsK*/*ftsK*$^+$ strain produced aerial hyphae with 5% anucleate spores. Thus, about two-thirds of the segregation phenotype associated with the *ftsK* truncation mutation was complemented. The Δ*smc*/*smc*$^+$ strain produced aerial hyphae that produced 3% anucleate spores, indicating that 50% of the phenotype associated with the mutation was complemented. Our complementation data suggest that the observed defects in segregation resulted, at least in part, from the introduced *ftsK* and *smc* insertion-deletion mutations (see additional complementation results below). At least one promoter, active in aerial hyphae, is present on the DNA inserts used for genetic complementation. However, proper temporal and spatial expression may require that the genes be located in their native chromosomal locations.

Δ*smc* Δ*ftsK*, Δ*smc* Δ*parB*, and Δ*ftsK* Δ*parB* double mutants have more-severe developmental defects. For the construction of double mutants, we used Δ*ftsK* mutant JM148 (*aphI* inserted in the same orientation as *ftsK′*) because the two mutants with either orientation of the marker had the same phenotype (Table 4). The Δ*smc* Δ*ftsK*, Δ*smc* Δ*parB*, and Δ*ftsK* Δ*parB* double mutants were constructed by transformation using DNA prepared from one mutant strain and using a second mutant as the recipient (Table 1). The double mutant strains were readily isolated, which indicated that the three double mutants were not synthetic lethal combinations. Macroscopically, these double mutants had a wild-type appearance without any obvious growth delay and formed robust gray aerial mycelia (Fig. 1D), although they all displayed colony heterogeneity relative to what was seen for the wild-type strain. Thus, the double mutants did not even have a synthetic sick phenotype.

DNA segregation did not appear to be affected in vegetative hyphae of the double mutants (data not shown). Observations by phase-contrast microscopy revealed aerial hyphae containing spores that were heterogeneous in size and shape compared to those of the single mutants or the wild type. In addition, Fig. 2E to G illustrates that spore chains in the double mutants had defects in developmental DNA partitioning, and the segregation defect in each strain was quantified (Table 4). The Δ*smc* Δ*ftsK* mutant produced aerial hyphae containing 13% anucleate spores, similar to those of the Δ*ftsK* strain (Fig. 2E). Therefore, additive effects of the mutations were not seen when combining the loss of a condensation gene (7%) with the segregation gene (15%). Interestingly, the Δ*ftsK* Δ*parB* mutant also was only 13% anucleate, which again indicated that this strain did not have segregation defects additive to those observed for the Δ*ftsK* (15%) and Δ*parB* (13%) single

mutant strains (Fig. 2G and Table 4). It seems that without the function of the two DNA-partitioning and segregation genes, *S. coelicolor* still can disseminate its DNA just as well as the most defective single mutant. In contrast, the Δ*smc* Δ*parB* mutant produced aerial hyphae containing 24% anucleate spores (Fig. 2F), slightly more than the additive effect (19%) of each individual gene loss (Table 4). Commensurate with the rise in the segregation defect, the Δ*smc* Δ*parB* mutant had a more defective developmental phenotype than the other double mutants. Aerial hyphae of the Δ*smc* Δ*parB* mutant contained more spore compartments with altered shapes and sizes. This observation, along with the single mutant data, suggested that there was a phenotypic effect when both a partitioning and a condensation gene in *S. coelicolor* were deleted, indicating genetic overlap or interaction.

In order to verify that the phenotypes in the double mutants resulted from the introduced mutations, genetic complementation analyses were completed with the low-copy-number plasmids bearing *smc* or *ftsK* or an integrated copy of *parB* (Table 4). Complementation data for the double mutant strains suggest that the phenotypes were linked to the mutations introduced by transformation into the Δ*smc* mutant. The Δ*smc* Δ*ftsK*/*ftsK*$^+$ strain produced aerial hyphae containing spores that were 7% anucleate, which indicates the that *ftsK* truncation mutation was completely complemented. The Δ*smc* Δ*parB*/*parB*$^+$ strain produced aerial hyphae that contained 6% anucleate spores, also indicating complete complementation. Finally, the Δ*ftsK* Δ*parB*/*ftsK*$^+$ strain produced aerial hyphae with 16% anucleate spores, which is similar to the 13% anucleate spores in aerial hyphae of the Δ*parB* strain. Complementation data suggest that the introduced second mutation was responsible for the observed phenotypes compared to the single mutant strains.

A Δ*smc* Δ*parB* Δ*ftsK* triple mutant is viable and does not have as severe of a developmental segregation defect as a Δ*smc* Δ*parB* double mutant. The Δ*smc* Δ*parB* Δ*ftsK* triple mutant was easily isolated by transformation with DNA prepared from a Δ*parB* strain and using the Δ*smc* Δ*ftsK* strain as the recipient. Macroscopically, the triple mutant showed no obvious growth delay and produced a robust gray aerial mycelium (Fig. 1D), but an elevation in colony heterogeneity was evident. Mutations in the three genes did not result in a synthetic lethal or synthetic sick phenotype.

Using phase-contrast microscopy, the spores of the Δ*smc* Δ*parB* Δ*ftsK* strain appeared heterogeneous in shape and size, most like those of the Δ*smc* Δ*parB* strain (Fig. 2H). Segregation did not appear to be affected in vegetative hyphae of the triple mutant (data not shown). Surprisingly, determination of the segregation phenotype for the triple mutant indicated that only 10% of the spores were anucleate (Table 4). The number of anucleate spores in aerial hyphae for the Δ*smc* Δ*parB* Δ*ftsK* strain was not the total sum of each single mutant combined (34%). It was not even as poor as the most severe phenotype of the double mutant strains (Δ*smc* Δ*parB* strain, 24%). Without all three of these genes, 90% of the spores still received some genomic material. This observation suggests that there must be considerable redundancy, and another unidentified system for developmental DNA segregation must function in this filamentous organism.

We performed genetic complementation analyses with the low-copy-number plasmids bearing *smc* or *ftsK* (Table 4). In particular, the complementation strain with the genotype Δ*smc* Δ*parB* Δ*ftsK*/*ftsK*$^+$ produced aerial hyphae with an increase in the number of anucleate spores to 27%, which was similar to the Δ*smc* Δ*parB* phenotype of 24% (Table 4). This verified that the introduced Δ*ftsK* truncation mutation was responsible for partially alleviating the segregation defects in the Δ*smc* Δ*parB* strain. Therefore, introducing a functional copy of *ftsK* back into the triple mutant made the genome segregation phenotype worse, suggesting that these genes interact genetically.

The fact that only 10% of triple mutant spores were anucleate prompted us to test if the viability of the spores was more adversely affected and the percent anucleate values were misleading. The viability of spores plated on MM supplemented with glucose was compared for the most pertinent strains. Wild-type strain produced spore compartments that were 49% viable. Although the Δ*ftsK* truncation and Δ*smc* Δ*parB* mutants have significant amounts of anucleate spores (15% and 24%, respectively), surprisingly, the viabilities of those produced were equal to or slightly higher than those of the wild type, respectively. In contrast, spores of the triple mutant were 12.5% viable, a level one-forth of that of the wild type. Although 90% of the spores in the triple mutant receive some genetic material, they are fourfold less fit than the wild type.

FtsK-EGFP localizes between nucleoids of aerial hyphae. *ftsK* was replaced by *ftsK-egfp* in the chromosome of the wild-type strain. This strain (RMD1) produced aerial hyphae containing spores with normal size and shape, as judged by phase-contrast microscopy. DNA segregation defects were not observed, as judged by fluorescence microscopy (data not shown). We concluded that the FtsK-EGFP fusion protein was functional.

Localization of FtsK-EGFP was analyzed at several time points during the life cycle, and FtsK-EGFP foci were apparent at both early vegetative and early aerial hyphae stages of growth. FtsK-EGFP was localized as distinct foci at several places within young germ tubes growing out of spores (Fig. 3A). Distinct gaps in the propidium iodide staining were repeatedly observed, and FtsK-EGFP foci coincided with those gaps in staining. This result suggested that DNA segregation could be occurring during the outgrowth of newly germinated spores and that there was a role for FtsK in this process. However, gaps in the propidium iodide staining were observed for *ftsK* mutants as well, indicating that the gaps in staining were not solely caused by the action of FtsK (data not shown). Although we attempted to stain membranes and cross-walls with unsatisfactory results, we assume that at least some gaps in DNA result from vegetative cross-walls. In addition, FtsK-EGFP localized as foci or bands in reproductive aerial hyphae prior to the formation of sporulation septa (Fig. 3B). The ladder-like pattern in the aerial hyphae was similar to what was observed for FtsZ localization (17, 46). These data indicated that FtsK localized to evenly spaced positions, as expected if it were to have a role in correctly positioning the nucleoids into prespore compartments before the DNA becomes trapped by the invaginating septa. Similar FtsK localization during synchronous septation in aerial hyphae has been reported independently (1, 53). In addition, we also observed potentially

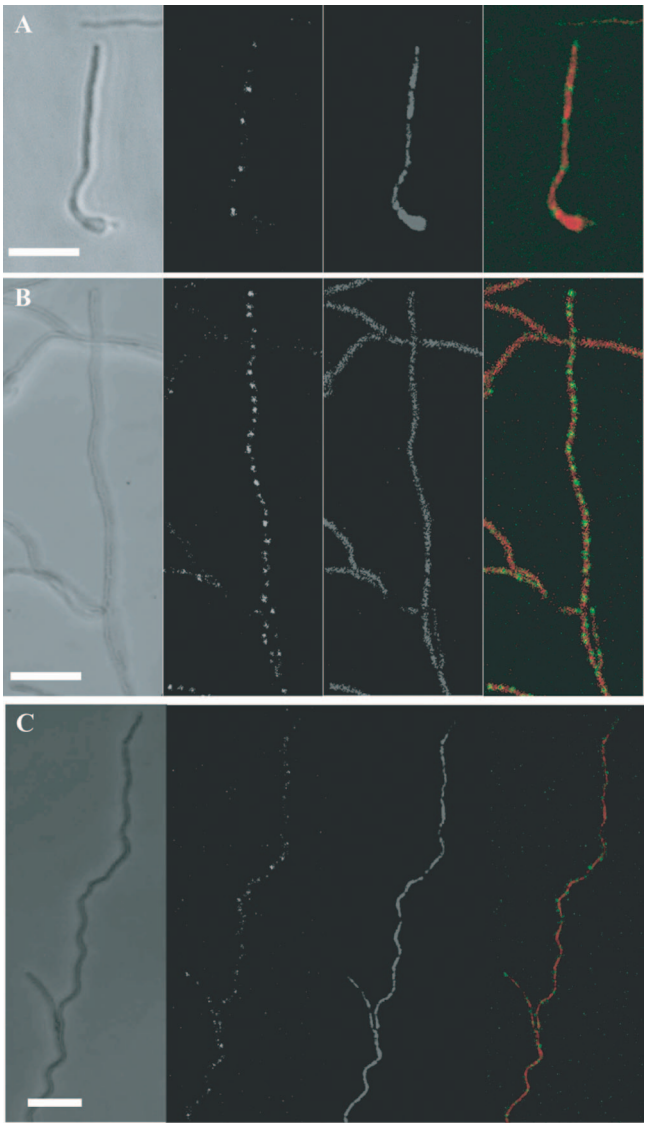

FIG. 3. FtsK-EGFP and SMC-EGFP fusion protein localization in vegetative and reproductive hyphae. Coverslips were inoculated and hyphae grown for 1 to 3 days on MS agar, fixed, and stained with propidium iodide. In each panel, representative hyphae are shown as phase-contrast and fluorescent images as observed by scanning laser confocal microscopy. From left to right, panels contain phase-contrast, EGFP, and DNA images and a merge of the two fluorescent images. (A) FtsK-EGFP localized in a vegetative filament newly emerging from a spore (lower right; 1 day of growth). (B) FtsK-EGFP localized in a regular pattern in a predivisional aerial filament just prior to prespore formation (long, central filament oriented with long axis of panel; 2 days of growth). (C) The SMC-EGFP fusion protein had an irregular punctuate pattern of localization in a predivisional aerial filament (2 to 3 days of growth). SMC-EGFP foci are not uniformly distributed, nor are they associated with every nucleoid. Bar: 7 μm.

helical structures that preceded the appearance of the evenly spaced ladder-like arrays, as reported by Wang et al. (53).

SMC-EGFP is localized in a punctuate pattern in aerial hyphae. *smc* was replaced by *smc-egfp* in the chromosome of the wild-type strain. This strain (RMD2) produced aerial hyphae containing spores with normal size and shape, as judged by phase-contrast microscopy. DNA segregation defects were not observed, as judged by fluorescence microscopy (data not shown). We concluded that the SMC-EGFP fusion protein was functional.

We anticipated that SMC might bind to every chromosome, helping to condense the DNA into nucleoids during genome segregation into prespore compartments. However, SMC-EGFP foci were not uniformly positioned and seemed to localize in a punctate pattern only in predivisional aerial hyphae. The foci were not observed to be associated with every nucleoid, nor with any particular region of the aerial filament (Fig. 3C). SMC-EGFP signal was not observed at any other time in the life cycle. Similar observations were made using immunofluorescence microscopy and an SMC-specific antibody (28a), indicating that the SMC-EGFP fusion did reflect the behavior of native SMC.

***scpA* and *scpB* mutants cause DNA condensation defects.** SMC functions in association with non-SMC proteins called ScpA and ScpB (*s*egregation and *c*ondensation *p*rotein) (32, 47). These proteins (MukEF) may regulate the SMC (MukB) association with DNA (33, 41). *scpA* (SCO1770) is 795 bp and is predicted to encode a 264-amino-acid protein and *scpB* (SCO1769) is 672 bp and is predicted to encode a 223-amino-acid protein (Fig. 1C). ScpA and ScpB are approximately 27% and 32% identical, respectively, to the *B. subtilis* homologues. The genes encoding ScpA and ScpB are adjacent and are likely to be cotranscribed with SCO1768, predicted to encode a pseudouridine synthase (Fig. 1C). Plasmids were constructed containing deletion-insertion mutations for SCO1768, *scpA*, and *scpAB* marked with an apramycin resistance cassette (Table 2). These mutations were introduced individually into the chromosome by conjugation, and marker replacement strains were readily isolated (Table 1), indicating that these genes are not essential for growth or viability. These strains produced normal gray, aerial mycelia characteristic of the wild-type strain (data not shown).

Deletion of *rluD*, coding for one of the many pseudouridine synthases in *E. coli*, causes a growth rate defect (20). Because *scpB* and SCO1768 overlap by 1 base and mutations in *scpA* or *scpB* were likely to have polar effects on the expression of SCO1768, we isolated a SCO1768 mutant to determine its phenotype in *S. coelicolor*. The introduced mutation for SCO1768 did not have an obvious effect on the growth rate, nor did it have a DNA segregation or condensation phenotype (data not shown). We conclude that the phenotypic effects observed for the Δ*scpA* or Δ*scpAB* mutants resulted from the deletion of those genes.

We anticipated that the *scpA* or *scpAB* mutants might have a segregation phenotype similar to that observed for the *smc* mutant. However, the observed frequency of anucleate spores was 1% (Table 5), insignificantly higher than that of the wild type (0.8%) and less than that of the *smc* deletion-insertion mutant (7%) (Table 4). Instead, a substantial fraction of nucleoids of the Δ*scpA* and Δ*scpAB* strains had an altered morphology in sporulating aerial hyphae (Fig. 4). Certain nucleoids did not follow the contours of the spore compartment and contain two lobes of DNA, a phenotype we have called "bilobed." In late aerial filaments, 15% of spores in the Δ*scpA* strain and 26% of spores in the Δ*scpAB* strain were bilobed (Table 5). In contrast, bilobed spores were not observed in the wild-type strain. Although the isolated deletion of *scpA* might be polar

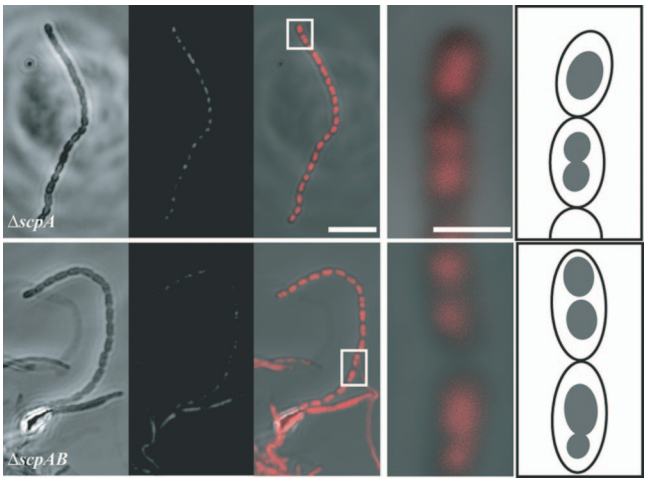

FIG. 4. The *scpA* and *scpAB* mutants have a bilobed nucleoid phenotype. Phase-contrast and fluorescent images of the same fields were taken by scanning laser confocal microscopy. Coverslips were inoculated and grown for 1 to 3 days on MS agar, fixed, and stained with propidium iodide. In each panel, phenotypes of representative aerial hyphae are shown as phase-contrast and fluorescent image pairs, followed by a merged image. For the merged images, the areas in the white boxes are enlarged and a cartoon interpretation is provided. (A) Images of Δ*scpA* (RMD18) showing spores with DNA appearing bilobed, unlike wild-type spores. (B) Images of Δ*scpAB* spores (RMD19) also appearing to have a bilobed DNA pattern. Bar: 7 μm.

on the expression of *scpB*, deleting both genes resulted in a higher frequency of bilobed spores, indicating that some *scpB* must be expressed in the *scpA* mutant. Genetic complementation experiments indicated that the observed nucleoid morphology defect was the result of the introduced deletion-insertion mutation for *scpA* or *scpAB*. Introduction of pRMD11, containing *scpAB*$^+$ and SCO1768, substantially reduced the occurrence of bilobed spores in the mutants (Table 5).

Because ScpA and ScpB are thought to regulate the interaction of SMC with DNA, we were interested in learning the phenotypes obtained when combining *scpA* or *scpAB* mutations with *smc* (Table 1). The data suggest that deleting *smc* in the *scpA* or *scpAB* mutant backgrounds combines their effects. While bilobed spores were not observed for the Δ*smc* mutant, aerial hyphae of the Δ*smc* Δ*scpA* double mutant produced 4% anucleate spores, and an additional 14% had a bilobed nucleoid morphology (Table 5). Aerial hyphae of the Δ*smc* Δ*scpAB* triple mutant produced 3% anucleate spores, and an additional 17% had a bilobed nucleoid morphology. An approximately similar number of spore compartments were affected in the triple mutant compared to the *scpAB* double mutant; however, the percentage of bilobed spores decreased and the percentage of anucleate spores increased. The data are consistent with an interpretation that ScpA and/or ScpB has functions in addition to regulating SMC activity.

DISCUSSION

***smc* and chromosome partitioning.** In this study, we described the isolation of an *smc* mutant. The main defect observed was in segregation, not in DNA condensation. The magnitude of the segregation defect in the *smc* mutant was modest, resulting in 7% anucleate prespore compartments, less than 10-fold more than that of the wild-type parent. The assembly of SMC condensation complexes presumably functions to compact and help pull the linear genome into the space available in prespore compartments. Consistent with the expected function and genetic defect, SMC-EGFP foci form in irregular patterns along aerial hyphae at a stage prior to when synchronous septation occurred and nucleoids were condensed. These results may suggest that nucleoid condensation in adjacent compartments of aerial hyphae is nonsynchronous. Alternatively, SMC-EGFP may not aggregate to discrete foci that can be visualized easily. SMC-EGFP foci were not observed in vegetative hyphae or in prespore compartments (i.e., postseptation). This could indicate that expression is developmentally regulated and SMC is present in a low concentration in vegetative hyphae, where DNA is not condensed, or early aerial hyphae, before DNA segregation occurs. Further regulation may be at the level of activity. SMC may only transiently and dynamically localize at points in the life cycle, such as when particular DNA sequences must be condensed in the maturing spore compartments. Similar results for the segregation phenotype of an *smc* mutant and SMC localization have been obtained independently (28a).

***ftsK* and chromosome partitioning.** In this study, we also described the isolation of mutants with different deletion-insertion mutations for *ftsK*. Consistent with two recent studies (1, 53), genome segregation during spore formation was not as appreciably affected as anticipated with an *ftsK* null mutation [Δ*ftsK*::*acc(3)IV*]. Spores with reduced DNA content were readily apparent, but anucleate spores were observed at the same level as for the wild type. Other *ftsK* mutants described here (Δ*ftsK*::*aphI* mutants) harbor a mutant allele (*ftsK′*) lacking the region encoding the DNA motor domain but still have the potential to produce a truncated protein of 203 native amino acids containing several N-terminal membrane-spanning segments (three out of four segments). In contrast, the truncation of *ftsK* resulted in a more deleterious segregation phenotype producing 15% anucleate spores, ~20-fold higher than that of the wild type. Interestingly, despite the obvious increase in missegregation, the spores produced did not suffer a dramatic loss of fitness and were as viable as the wild type when germination and growth were tested on MM with glucose (46% versus 49%, respectively).

Except for segregation in the mutant with a truncated *ftsK* gene, everything else in growth and development—aerial mycelium formation, septation, septum spacing, spore maturation

TABLE 5. Quantitative analysis of *scp* mutant genome segregation and nucleoid morphology phenotypes during spore formation

Strain or mutation	% Anucleate spores[a]	% Bilobed spores[a]	Total no. of spores
Wild type	0.8	0	2,233
Δ*scpA*::*acc(3)IV*	1	15	1,797
Δ*scpAB*::*acc(3)IV*	1	26	1,787
Δ*scpA*::*acc(3)IV*/*scpAB*$^+$	1	2	1,790
Δ*scpAB*::*acc(3)IV*/*scpAB*$^+$	1	4	1,626
Δ*smc*::*hyg* Δ*scpA*::*acc(3)IV*	4	14	3,589
Δ*smc*::*hyg* Δ*scpAB*::*acc(3)IV*	3	17	3,148

[a] One hundred random spore chains were quantified and the percentages of anucleate and bilobed spores were determined. All spores were considered regardless of the compartment size.

(compartment rounding up), and spore pigment production—appeared to be normal. In addition, FtsZ-EGFP localized correctly in the *frsk* mutant, indicating that the C-terminal motor domain is not required for, and the N-terminal fragment did not interfere with, Z ring formation (data not shown). Thus, FtsK′ does not appear to be pleiotropically poisoning a central process such as the general secretion/membrane insertion pathway. A segregation phenotype is what would be predicted based on previous work with other organisms, and that is in fact the phenotype observed. Because the phenotype of *ftsK′* is different from the loss of the entire gene, we think that the results are consistent with the interpretation that the FtsK′ fragment (truncated cleanly between the third and fourth predicted transmembrane helices) associates with the components with which FtsK may normally interact. We predict that FtsK′ is where it is supposed to be but that it is unable to transport DNA. We conclude that the FtsK motor domain is important for proper genome segregation during prespore formation and that the N-terminal 203-amino-acid FtsK′ must interact with some component during prespore formation. The expression of FtsK′ did not result in a dominant-negative phenotype, as the genome segregation defect could be complemented by expression of *ftsK*$^+$ from a low-copy-number plasmid (Table 4). In speculation, this may indicate that the first three transmembrane segments of the FtsK/SpoIIIE family are important for the majority of normal function and that the final transmembrane segment is responsible for positioning the DNA motor domain on the correct side of the membrane.

Consistent with the expected function of moving DNA trapped by invaginating septa, FtsK-EGFP foci and bands were observed to form in regular ladder-like patterns along aerial hyphae at a stage when synchronous septation occurred and the nucleoids would become condensed. Our data support similar observations from two other recent studies (1, 53). In addition, FtsK-EGFP foci were observed in germ tubes during spore outgrowth, suggesting that FtsK might function in the vegetative hyphae, presumably moving DNA trapped when forming the widely spaced vegetative cross-walls.

Genetic interactions between segregation and condensation genes. We combined our mutations for *smc* and truncated *ftsK* (*ftsK′*) with each other and that of *parB*. ParB is responsible for organizing the origin proximal-region of the linear chromosomes into nucleoprotein complexes that are synchronously positioned at regularly spaced distances to help ensure that copies of the genome are captured within each prespore compartment (25, 26). A *parB* mutant produces 13% anucleate spores, ~20-fold higher than the wild type (Table 4) (28). Combining *ftsK′* with *smc* or *parB* mutations did not give an additive effect, and the production of anucleate spores was approximately 13% for both double mutants, similar to the worst single mutant. In contrast, *smc* and *parB* are in two pathways, as combining the two mutations led to 24% anucleate spores, approximately the sum of the phenotypes for each single mutant. Despite the obvious increase in missegregation, the spores produced by an *smc parB* mutant did not suffer a dramatic loss of fitness and were slightly more viable than the wild type when germination and growth were tested on MM with glucose.

The most interesting result was observed when we isolated an *smc parB ftsK′* triple mutant. We anticipated that removing *ftsK*$^+$ would exacerbate the segregation phenotype. Instead, introducing the *ftsK′* mutation into the *smc parB* background improved the ability to segregate genomic material into prespore compartments (24% anucleate for the double mutant versus 10% for the triple mutant). We confirmed the alteration in the segregation phenotype resulted from the introduced *ftsK′* mutation. Genetic complementation of *ftsK′* (*smc parB ftsK′*/*ftsK*$^+$) resulted in a phenotype similar to that for the *smc parB* double mutant (27% anucleate spores). Our data indicate that there must be considerable redundancy and more genes that can provide backup function in segregation when *smc*, *parB*, and *ftsK* are inactive, or we are left to conclude that unassisted postreplication diffusion of nucleoids accounts for the even distribution of genomes during development. In the absence of the three well-characterized genes involved in bacterial genome segregation, normally resulting in lethal or synthetic lethal phenotypes when combined in rod-shaped bacteria, an impressive 90% of the spore compartments receive at least some genomic material. A portion of those genomes in spore compartments must be complete or nearly complete copies, as the triple mutant spores are approximately 25% as viable as those produced by the wild-type parent when tested on MM with glucose. Certainly, some genomes must be guillotined by the septa and account for the loss of viability.

When normal genome segregation is disturbed by the loss of ParB and SMC, the FtsK DNA motor domain may clear trapped genomes to the "wrong" side of invaginating septa too quickly, resulting in 24% anucleate compartments. When FtsK′ is expressed, a less efficient backup system(s) may function in the *smc parB* mutant. The less efficient redundant system is able to eventually segregate genomes into a larger proportion of prespore compartments when the strong FtsK motor is not rapidly clearing DNA from invaginating septa. A better understanding of segregation will require additional analysis. One obvious candidate might be the recently described FtsK-like protein SffA, although the functions of SffA and FtsK did not appear to overlap (1). Due to the considerable redundancy demonstrated here, the contributions of SffA may not be apparent until they are tested in *smc parB* or *smc parB ftsK′* mutants. Related to the subtle phenotype of an *sffA* mutant (1), infrequent spores with double the DNA intensity were not observed adjacent to anucleate spores in any of the mutants described here. Likewise, another *ftsK*-like gene (SCO4508) could be a candidate and was tested for a role in segregation (53), but its function may not be apparent until combined with the other genes tested here. Due to the lack of compatible markers, we have yet to test the effect of *ftsK*-null allele when combined with *smc parB*. Finally, we anticipate that additional components influencing segregation might be cytoskeletal proteins MreB or Mbl (9a, 16, 49) or genes under the regulation of SsgC (40).

Genetic instability of the linear genome. A recent study with an *ftsK*-null mutant reported that portions of the right end of the chromosome were frequently lost in some colonies during routine propagation of the mutant strain (53). The interpretation of that study was that loss of FtsK resulted in an increase in genome instability. We and Ausmees et al. (1) also observed an increase of colony heterogeneity with *ftsK* mutants. However, we note that an increase in genome instability resulted in most of our mutants. We believe that increased genome insta-

bility is not specific for the loss of FtsK sweeping the arms of the linear chromosome from being strangled and lost but rather is a property of DNA segregation mutants in general. To test if the segregation mutants in this study suffered unanticipated genetic loss, we subjected all of our strains to Southern blot hybridization analyses using the inserts of two nonoverlapping cosmids as probes to see if there were any observable differences in the *cmlR* (SCO7526) region near the right end of the chromosome. The strains from this study did not have observable deletions or rearrangements (data not shown).

Nucleoid morphology defects in a *scpAB*-null mutant. We anticipated that mutants for genes encoding non-SMC segregation and condensation proteins ScpA and ScpB would have a phenotype similar to the *smc* mutant but perhaps more modest (32). These proteins were thought to interact with SMC to influence the interaction of SMC with DNA and are required to form higher-order structures involved in genome condensation. However, the phenotype of the *smc* mutant is distinct from those of the *scpA* and *scpAB* mutants. The loss of *scpA* or *scpAB* mainly affected the morphology of the condensed nucleoid and did not give rise to a significant segregation defect. Isolation of *smc scpA* and *smc scpAB* mutants indicated that the phenotypes of the double and triple mutants were additive. These mutants have both a segregation phenotype (*smc*) and a nucleoid morphology phenotype (*scpAB*). We speculate that in addition to the normal interaction with SMC, the nucleoid morphology perturbation might be the result of ScpA and ScpB interacting with additional proteins required for and regulating processes associated with condensation and genome organization. The SMC-ScpA-ScpB complex was shown to have a role in DNA repair and gene regulation in *B. subtilis* (10). Those authors proposed that these roles are evolutionarily conserved and our data may agree.

Finally, the bilobed morphology of the nucleoids observed for the *scpA* and *scpAB* mutants could offer insight into the way the genome is stored in the quiescent spore. The genome in streptomycetes is a linear DNA molecule with TIRs. For vegetative hyphae, evidence suggests that the TIRs are held in association near each other (58), and perhaps the ends are also normally in association in the spore. In the *scpAB* mutants, the TIRs may no longer be closely associated, revealing two independently folding domains of the nucleoid. Alternatively, a DNA replication checkpoint may have failed and the mutant prespore compartments might undergo an additional round of DNA replication. Other possibilities exist and we will be exploring the problem in future studies.

ACKNOWLEDGMENTS

We thank Agnieszka Kois and Jolanta Zakrzewska-Czerwińska for communicating their work to us prior to publication. We thank Aimee Belanger for constructing plasmids pAEB228 and pAEB232, Dagmara Jakimowicz for H24*parB-egfp*, Keith Chater for *parB* mutant strains, Bertolt Gust for technical advice, and Patrick Viollier for helpful discussions.

This work was supported, in part, by grant GM56915 from the National Institutes of Health (to J.R.M.).

REFERENCES

1. **Ausmees, N., H. Wahlstedt, S. Bagchi, M. A. Elliot, M. J. Buttner, and K. Flardh.** 2007. SmeA, a small membrane protein with multiple functions in *Streptomyces* sporulation including targeting of a SpoIIIE/FtsK-like protein to cell division septa. Mol. Microbiol. **65:**1458–1473.
2. **Barre, F. X.** 2007. FtsK and SpoIIIE: the tale of the conserved tails. Mol. Microbiol. **66:**1051–1055.
3. **Bentley, S. D., K. F. Chater, A. M. Cerdeno-Tarraga, G. L. Challis, N. R. Thomson, K. D. James, D. E. Harris, M. A. Quail, H. Kieser, D. Harper, A. Bateman, S. Brown, G. Chandra, C. W. Chen, M. Collins, A. Cronin, A. Fraser, A. Goble, J. Hidalgo, T. Hornsby, S. Howarth, C. H. Huang, T. Kieser, L. Larke, L. Murphy, K. Oliver, S. O'Neil, E. Rabbinowitsch, M. A. Rajandream, K. Rutherford, S. Rutter, K. Seeger, D. Saunders, S. Sharp, R. Squares, S. Squares, K. Taylor, T. Warren, A. Wietzorrek, J. Woodward, B. G. Barrell, J. Parkhill, and D. A. Hopwood.** 2002. Complete genome sequence of the model actinomycete *Streptomyces coelicolor* A3(2). Nature **417:**141–147.
4. **Bierman, M., R. Logan, K. O'Brien, E. T. Seno, R. N. Rao, and B. E. Schoner.** 1992. Plasmid cloning vectors for the conjugal transfer of DNA from *Escherichia coli* to *Streptomyces* spp. Gene **116:**43–49.
5. **Bignell, C., and C. M. Thomas.** 2001. The bacterial ParA-ParB partitioning proteins. J. Biotechnol. **91:**1–34.
6. **Bigot, S., V. Sivanathan, C. Possoz, F. X. Barre, and F. Cornet.** 2007. FtsK, a literate chromosome segregation machine. Mol. Microbiol. **64:**1434–1441.
7. **Breier, A. M., and A. D. Grossman.** 2007. Whole-genome analysis of the chromosome partitioning and sporulation protein Spo0J (ParB) reveals spreading and origin-distal sites on the *Bacillus subtilis* chromosome. Mol. Microbiol. **64:**703–718.
8. **Chen, N., A. A. Zinchenko, Y. Yoshikawa, S. Araki, S. Adachi, M. Yamazoe, S. Hiraga, and K. Yoshikawa.** 2008. ATP-induced shrinkage of DNA with MukB protein and MukBEF complex of *Escherichia coli*. J. Bacteriol. **190:** 3731–3737.
9. **Cui, Y., Z. M. Petrushenko, and V. V. Rybenkov.** 2008. MukB acts as a macromolecular clamp in DNA condensation. Nat. Struct. Mol. Biol. **15:** 411–418.

9a. **Defeu Soufo, H. J., and P. L. Graumann.** 2003. Actin-like proteins MreB and Mbl from *Bacillus subtilis* are required for bipolar positioning of replication origins. Curr. Biol. **13:**1916–1920.

10. **Dervyn, E., M. F. Noirot-Gros, P. Mervelet, S. McGovern, S. D. Ehrlich, P. Polard, and P. Noirot.** 2004. The bacterial condensin/cohesin-like protein complex acts in DNA repair and regulation of gene expression. Mol. Microbiol. **51:**1629–1640.
11. **Dorazi, R., and S. J. Dewar.** 2000. Membrane topology of the N-terminus of the *Escherichia coli* FtsK division protein. FEBS Lett. **478:**13–18.
12. **Ebersbach, G., and K. Gerdes.** 2005. Plasmid segregation mechanisms. Annu. Rev. Genet. **39:**453–479.
13. **Elliot, M. A., M. J. Buttner, and J. R. Nodwell.** 2008. Multicellular development in *Streptomyces*, p. 419–438. *In* D. E. Whitworth (ed.), Myxobacteria: multicellularity and differentiation. ASM Press, Washington, DC.
14. **Errington, J., H. Murray, and L. J. Wu.** 2005. Diversity and redundancy in bacterial chromosome segregation mechanisms. Philos. Trans. R. Soc. Lond. B **360:**497–505.
15. **Flärdh, K.** 2003. Growth polarity and cell division in *Streptomyces*. Curr. Opin. Microbiol. **6:**564–571.
16. **Gitai, Z., N. A. Dye, A. Reisenauer, M. Wachi, and L. Shapiro.** 2005. MreB actin-mediated segregation of a specific region of a bacterial chromosome. Cell **120:**329–341.
17. **Grantcharova, N., U. Lustig, and K. Flärdh.** 2005. Dynamics of FtsZ assembly during sporulation in *Streptomyces coelicolor* A3(2). J. Bacteriol. **187:** 3227–3237.
18. **Graumann, P. L.** 2001. SMC proteins in bacteria: condensation motors for chromosome segregation? Biochimie **83:**53–59.
19. **Gust, B., G. Chandra, D. Jakimowicz, T. Yuqing, C. J. Bruton, and K. F. Chater.** 2004. Lambda red-mediated genetic manipulation of antibiotic-producing *Streptomyces*. Adv. Appl. Microbiol. **54:**107–128.
20. **Gutgsell, N. S., M. Del Campo, S. Raychaudhuri, and J. Ofengand.** 2001. A second function for pseudouridine synthases: a point mutant of RluD unable to form pseudouridines 1911, 1915, and 1917 in *Escherichia coli* 23S ribosomal RNA restores normal growth to an RluD-minus strain. RNA **7:**990–998.
21. **Hirano, M., and T. Hirano.** 2006. Opening closed arms: long-distance activation of SMC ATPase by hinge-DNA interactions. Mol. Cell **21:**175–186.

21a. **Hirano, T.** 1999. SMC-mediated chromosome mechanics: a conserved scheme from bacteria to vertebrates? Genes Dev. **13:**11–19.

22. **Hirano, T.** 2006. At the heart of the chromosome: SMC proteins in action. Nat. Rev. Mol. Cell Biol. **7:**311–322.
23. **Iyer, L. M., K. S. Makarova, E. V. Koonin, and L. Aravind.** 2004. Comparative genomics of the FtsK-HerA superfamily of pumping ATPases: implications for the origins of chromosome segregation, cell division and viral capsid packaging. Nucleic Acids Res. **32:**5260–5279.
24. **Jakimowicz, D., K. Chater, and J. Zakrzewska-Czerwińska.** 2002. The ParB protein of *Streptomyces coelicolor* A3(2) recognizes a cluster of *parS* sequences within the origin-proximal region of the linear chromosome. Mol. Microbiol. **45:**1365–1377.
25. **Jakimowicz, D., B. Gust, J. Zakrzewska-Czerwińska, and K. F. Chater.** 2005. Developmental-stage-specific assembly of ParB complexes in *Streptomyces coelicolor* hyphae. J. Bacteriol. **187:**3572–3580.

26. **Jakimowicz, D., P. Zydek, A. Kois, J. Zakrzewska-Czerwińska, and K. F. Chater.** 2007. Alignment of multiple chromosomes along helical ParA scaffolding in sporulating *Streptomyces* hyphae. Mol. Microbiol. **65:**625–641.
27. **Kieser, T., M. J. Bibb, M. J. Buttner, K. F. Chater, and D. A. Hopwood.** 2000. Practical *Streptomyces* genetics. The John Innes Foundation, Norwich, England.
28. **Kim, H.-J., M. J. Calcutt, F. J. Schmidt, and K. F. Chater.** 2000. Partitioning of the linear chromosome during sporulation of *Streptomyces coelicolor* A3(2) involves an *oriC*-like *parAB* locus. J. Bacteriol. **182:**1313–1320.

28a. **Kois, A., M. Świątek, D. Jakimowicz, and J. Zakrzewska-Czerwińska.** 2009. SMC protein-dependent chromosome condensation during aerial hyphal development in *Streptomyces*. J. Bacteriol. **191:**310–319.

28b. **Koshland, D., and A. Strunnikov.** 1996. Mitotic chromosome condensation. Annu. Rev. Cell Dev Biol. **12:**305–333.

29. **Kuhstoss, S., and R. N. Rao.** 1991. A thiostrepton-inducible expression vector for use in *Streptomyces* spp. Gene **103:**97–99.
30. **Liu, G., G. C. Draper, and W. D. Donachie.** 1998. FtsK is a bifunctional protein involved in cell division and chromosome localization in *Escherichia coli*. Mol. Microbiol. **29:**893–903.
31. **MacNeil, D. J., K. M. Gewain, C. L. Ruby, G. Dezeny, P. H. Gibbons, and T. MacNeil.** 1992. Analysis of *Streptomyces avermitilis* genes required for avermectin biosynthesis utilizing a novel integration vector. Gene **111:**61–68.
32. **Mascarenhas, J., J. Soppa, A. V. Strunnikov, and P. L. Graumann.** 2002. Cell cycle-dependent localization of two novel prokaryotic chromosome segregation and condensation proteins in *Bacillus subtilis* that interact with SMC protein. EMBO J. **21:**3108–3118.
33. **Mascarenhas, J., A. V. Volkov, C. Rinn, J. Schiener, R. Guckenberger, and P. L. Graumann.** 2005. Dynamic assembly, localization and proteolysis of the *Bacillus subtilis* SMC complex. BMC Cell Biol. **6:**28.
34. **Massey, T. H., C. P. Mercogliano, J. Yates, D. J. Sherratt, and J. Löwe.** 2006. Double-stranded DNA translocation: structure and mechanism of hexameric FtsK. Mol. Cell **23:**457–469.
35. **McCormick, J. R., and R. Losick.** 1996. Cell division gene *ftsQ* is required for efficient sporulation but not growth and viability in *Streptomyces coelicolor* A3(2). J. Bacteriol. **178:**5295–5301.
36. **McCormick, J. R., E. P. Su, A. Driks, and R. Losick.** 1994. Growth and viability of *Streptomyces coelicolor* mutant for the cell division gene *ftsZ*. Mol. Microbiol. **14:**243–254.
37. **Miguélez, E. M., B. Rueda, C. Hardisson, and M. B. Manzanal.** 1998. Nucleoid partitioning and the later stages of sporulation septum synthesis are closely associated events in the sporulating hyphae of *Streptomyces carpinensis*. FEMS Microbiol. Lett. **159:**59–62.
38. **Nasmyth, K., and C. H. Haering.** 2005. The structure and function of SMC and kleisin complexes. Annu. Rev. Biochem. **74:**595–648.
39. **Niki, H., A. Jaffe, R. Imamura, T. Ogura, and S. Hiraga.** 1991. The new gene *mukB* codes for a 177 kD protein with coiled-coil domains involved in chromosome partitioning of *E. coli*. EMBO J. **10:**183–193.
40. **Noens, E. E., V. Mersinias, B. A. Traag, C. P. Smith, H. K. Koerten, and G. P. van Wezel.** 2005. SsgA-like proteins determine the fate of peptidoglycan during sporulation of *Streptomyces coelicolor*. Mol. Microbiol. **58:**929–944.
41. **Petrushenko, Z. M., C. H. Lai, and V. V. Rybenkov.** 2006. Antagonistic interactions of kleisins and DNA with bacterial condensin MukB. J. Biol. Chem. **281:**34208–34217.
42. **Ptacin, J. L., M. Nollmann, E. C. Becker, N. R. Cozzarelli, K. Pogliano, and C. Bustamante.** 2008. Sequence-directed DNA export guides chromosome translocation during sporulation in *Bacillus subtilis*. Nat. Struct. Mol. Biol. **15:**485–493.
43. **Redenbach, M., H. M. Kieser, D. Denapaite, A. Eichner, J. Cullum, H. Kinashi, and D. A. Hopwood.** 1996. A set of ordered cosmids and a detailed genetic and physical map for the 8 Mb *Streptomyces coelicolor* A3(2) chromosome. Mol. Microbiol. **21:**77–96.
44. **Ruban-Ośmiałowska, B., D. Jakimowicz, A. Smulczyk-Krawczyszyn, K. F. Chater, and J. Zakrzewska-Czerwińska.** 2006. Replisome localization in vegetative and aerial hyphae of *Streptomyces coelicolor*. J. Bacteriol. **188:**7311–7316.
45. **Sambrook, J., E. F. Fritsch, and T. Maniatis.** 1989. Molecular cloning: a laboratory manual, 2nd ed. Cold Spring Harbor Laboratory, Cold Spring Harbor, NY.
46. **Schwedock, J., J. R. McCormick, E. R. Angert, J. R. Nodwell, and R. Losick.** 1997. Assembly of the cell division protein FtsZ into ladder-like structures in the aerial hyphae of *Streptomyces coelicolor*. Mol. Microbiol. **25:**847–858.
47. **Soppa, J., K. Kobayashi, M. F. Noirot-Gros, D. Oesterhelt, S. D. Ehrlich, E. Dervyn, N. Ogasawara, and S. Moriya.** 2002. Discovery of two novel families of proteins that are proposed to interact with prokaryotic SMC proteins, and characterization of the *Bacillus subtilis* family members ScpA and ScpB. Mol. Microbiol. **45:**59–71.
48. Reference deleted.
49. **Srivastava, P., G. Demarre, T. S. Karpova, J. McNally, and D. K. Chattoraj.** 2007. Changes in nucleoid morphology and origin localization upon inhibition or alteration of the actin homolog, MreB, of *Vibrio cholerae*. J. Bacteriol. **189:**7450–7463.
50. **Strunnikov, A. V.** 2006. SMC complexes in bacterial chromosome condensation and segregation. Plasmid **55:**135–144.

50a. **Strunnikov, A. V.** 1998. SMC proteins and chromosome structure. Trends Cell Biol. **8:**454–459.

51. **Thanbichler, M., and L. Shapiro.** 2008. Getting organized—how bacterial cells move proteins and DNA. Nat. Rev. Microbiol. **6:**28–40.
52. **Virca, G. D., W. Northemann, B. R. Sheils, G. Widera, and S. Broome.** 1990. Simplified Northern blot hybridization using 5% sodium dodecyl sulfate. BioTechniques **8:**370–371.
53. **Wang, L., Y. Yu, X. He, X. Zhou, Z. Deng, K. F. Chater, and M. Tao.** 2007. Role of an FtsK-like protein in genetic stability in *Streptomyces coelicolor* A3(2). J. Bacteriol. **189:**2310–2318.
54. **Wildermuth, H., and D. A. Hopwood.** 1970. Septation during sporulation in *Streptomyces coelicolor*. J. Gen. Microbiol. **60:**51–59.
55. **Wildschutte, H.** 2000. Analysis of *smc* and *in vivo* transposon mutagenesis in *Streptomyces coelicolor*. MS thesis. Duquesne University, Pittsburgh, PA.
56. **Wu, L. J., and J. Erington.** 1997. Septal localization of the SpoIIIE chromosome partitioning protein in *Bacillus subtilis*. EMBO J. **16:**2161–2169.
57. **Wu, L. J., and J. Errington.** 1994. *Bacillus subtilis* spoIIIE protein required for DNA segregation during asymmetric cell division. Science **264:**572–575.
58. **Yang, M. C., and R. Losick.** 2001. Cytological evidence for association of the ends of the linear chromosome in *Streptomyces coelicolor*. J. Bacteriol. **183:**5180–5186.
59. **Yu, X.-C., E. K. Weihe, and W. Margolin.** 1998. Role of the C terminus of FtsK in *Escherichia coli* chromosome segregation. J. Bacteriol. **180:**6424–6428.